4th International Conference on Spacecraft Formation Flying Missions and Technologies
May 18-20, 2011
St. Hubert, Quebec, Canada

Novel Coordinate Transformation and Robust Cooperative Formation Control for Swarms of Spacecraft

Insu Chang[1], Soon-Jo Chung[1], Fred Y. Hadaegh[2]
[1]*University of Illinois at Urbana-Champaign, Urbana, USA;*
[2]*Jet Propulsion Laboratory, California Institute of Technology, Pasadena, USA*

Abstract
This paper presents a new coordinate transformation method for controlling a large number of spacecraft moving in elliptical orbits. A new coordinate transformation method for phase synchronization of spacecraft in relative elliptical orbits is introduced to effectively maintain desired formation patterns. The proposed controller, which employs both the adaptive graph Laplacian matrix and the distance-based connectivity rule, synchronizes the relative motions of spacecraft with a guaranteed property of robustness. A complex time-varying network topology, constructed by the proposed controller, relaxes the standard requirement of consensus stability, even permitting stabilization on an arbitrary unbalanced graph. A challenging example of reconfiguring swarms of spacecraft shows the reliability of the coordinate transformation method and the effectiveness of the proposed phase synchronization controller.

1. Introduction

Spacecraft formation flying (SFF) has been extensively studied due to its potential applications in future space science missions such as stellar interferometry. Despite the benefits of SFF, there exist unique challenges in guidance, navigation, and control of SFF [1]. This paper focuses on a more challenging application of swarms of formation flying spacecraft [2]. The sheer number of spacecraft (1000s) involved in spacecraft swarms significantly complicates the formation control problem.

The objective of this paper is to introduce a new coordinate transformation method as well as a novel formation controller for swarms of spacecraft. There have been a variety of studies on SFF. Surveys of SFF guidance and control are given by [3, 4]. Various architectures for SFF were introduced in [5]. A leader-follower system has been the most popular method [6], and several types of decentralized coordinate-based control have also been extensively studied [7, 8]. Various linear and nonlinear control methods have been proposed (e.g., integrator backstepping control [9], passivity-based control [10], output feedback [11], adaptive control [12]). Based on [13], a combined controller for attitude and orbital motions of SFF was introduced in [8], which utilizes phase synchronization in circular motions. Exact nonlinear dynamics and cooperative control for SFF based on the adaptive Graph Laplacians and distance-based connectivity were introduced in [14] under the assumption that each spacecraft knows its desired trajectory explicitly.

We can summarize the main contributions of the paper as follows. First, the proposed coordinate transformation method and the phase angle shift method facilitate phase angle shifts in any elliptical orbits in three-dimensional (3D) space so that the motions of spacecraft in elliptical orbits can be described by the combination of *circular* and *sinusoidal* motions in a new coordinate system.

Second, the proposed phase synchronization controller, which is proven to be exponentially stabilizing the spacecraft trajectories, actively attempts to find time-varying tracking and diffusive coupling gains by means of the adaptive graph Laplacians and the distance-based connectivity method [14]. This way, a large number of spacecraft in a swarm of spacecraft can be effectively synchronized. The phase synchronization controller eliminates the need for having a balanced graph (i.e., the number of inputs for coupling is the same as that of outputs) for synchronization [15].

We investigate the effectiveness of the proposed methods by using a swarm of spacecraft rotating and reconfiguring in multiple concentric relative orbits.

The organization of this paper is as follows: In Section 3, the problem statement is presented. In Section 4, the new coordinate transformation method and the phase angle shift method are introduced. The proposed phase synchronization control law is given in Section 5. In Section 6, results of simulation are discussed. Finally, concluding remarks are given in Section 7.

3. Problem Statement

Suppose that there is a swarm of spacecraft consisting of p spacecraft whose individual dynamic model (jth agent ($1 \leq j \leq p$)) is given by the Euler-Lagrangian (EL) formulation

$$\mathbf{M}_j(\mathbf{q}_j)\ddot{\mathbf{q}}_j + \mathbf{C}_j(\mathbf{q}_j, \dot{\mathbf{q}}_j)\dot{\mathbf{q}}_j + \mathbf{G}_j(\mathbf{q}_j) = \boldsymbol{\tau}_j + \mathbf{D}_j(\mathbf{q}_j, \dot{\mathbf{q}}_j) \tag{1}$$

where $\mathbf{q}_j \in \mathbb{R}^n$, $\mathbf{M}_j(\mathbf{q}_j) \in \mathbb{R}^{n\times n}$, $\mathbf{C}_j(\mathbf{q}_j, \dot{\mathbf{q}}_j) \in \mathbb{R}^{n\times n}$, $\mathbf{G}_j(\mathbf{q}_j) \in \mathbb{R}^n$, $\boldsymbol{\tau}_j \in \mathbb{R}^n$, and $\mathbf{D}_j(\mathbf{q}_j, \dot{\mathbf{q}}_j) \in \mathbb{R}^n$ denote the states, the inertia matrix, the Coriolis/centrifugal forces, the gravitational force, the control input, and the non-conservative forces, respectively. Note that $\mathbf{C}_j(\mathbf{q}_j, \dot{\mathbf{q}}_j)$ is chosen such that $\dot{\mathbf{M}}_j(\mathbf{q}_j) - 2\mathbf{C}_j(\mathbf{q}_j, \dot{\mathbf{q}}_j)$ is skew-symmetric, which plays a critical role in stability proofs in this paper.
Note that the exact nonlinear dynamic models for chief and deputy spacecraft which include J_2 perturbation and atmospheric drag as disturbances can be found in [17].

We want to design a formation control and phase synchronization controller such that the spacecraft in a swarm can maintain their positions with bounded errors with respect to the desired trajectories in multiple concentric ellipses. In order to construct the desired trajectories, it is assumed that there is a pre-designated orbit leader spacecraft, which can be either a physical spacecraft or a virtual one. The orbit leader spacecraft is used for more systematic handling of the network (e.g., formation keeping, reconfiguration, etc.). Figure 1 shows two frames (the Earth Centered Inertial (ECI) and the Local Vertical and Local Horizontal (LVLH) frames) and a swarm of spacecraft moving in multiple concentric ellipses.

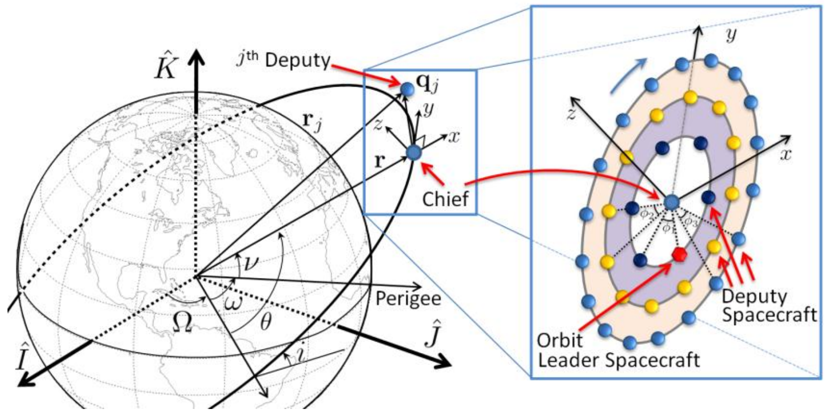

Fig. 1 Coordinate systems and spacecraft swarm in multiple concentric orbits

4. Periodic Relative Orbits (PROs)

In this paper, we consider periodic motions for the desired trajectory. The periodic motions, specifically in the LVLH frame, are called PROs. The PROs can be obtained from the solutions of the HCW equation [16]:

$$\begin{aligned} x_d(t) &= \dot{x}_0 / n s_{nt} - (3x_0 + 2\dot{y}_0)c_{nt} + 4x_0 + 2\dot{y}_0 / n \\ y_d(t) &= 2\{\dot{x}_0 / n c_{nt} + (3x_0 + 2\dot{y}_0 / n)s_{nt}\} - 3nt / 2(4x_0 + 2\dot{y}_0 / n) + (y_0 - 2\dot{x}_0 / n) \\ z_d(t) &= z_0 c_{nt} + \dot{z}_0 / n s_{nt} \end{aligned} \tag{3}$$

where $q_d = [x_d \quad y_d \quad z_d]^T$ denotes the relative motion of the desired trajectory and x_0, y_0, and z_0 denote the initial values of x_d, y_d, z_d that can be chosen arbitrarily. The time-varying variable $n = \sqrt{\mu / a^3}$ is the mean motion of the chief spacecraft.

In this paper, we assume that PROs are concentric with $(0,\ 0)$, the center of the LVLH frame. Therefore, the conditions for PROs without a drift in the LVLH frame are $\dot{y}_0 = -2nx_0$ and $\dot{x}_0 = ny_0 / 2$. By substituting the two condtions into Eq. (3), the periodic solutions without a drift in the LVLH frame can be expressed in a compact form as

$$x_d(t) = a_e s_{\psi_e}, \quad y_d(t) = 2a_e c_{\psi_e}, \quad z_d(t) = z_{\max} s_{\psi_z} \tag{4}$$

where $a_e = \sqrt{(\dot{x}_0 / n)^2 + (3x_0 + 2\dot{y}_0 / n)^2}$, $\psi_e = \psi - \psi_{e_0}$, $\psi = nt$, $\psi_{e_0} = \tan^{-1}((3nx_0 + 2\dot{y}_0) / \dot{x}_0)$, $z_{\max} = \sqrt{z_0^2 + (\dot{z}_0 / n)^2}$, $\psi_z = \psi + \psi_{z_0}$, and $\psi_{z_0} = \tan^{-1}(nz_0 / \dot{z}_0)$, respectively.

Note that the solutions describe elliptic orbits with the relative semimajor axis ($2a_e$), which is twice longer than the relative semiminor axis (a_e). The solutions in Eq. (5) will be used as desired trajectories of the orbit leader spacecraft.

5. New Coordinate Transformation and Phase Angle Shift in Elliptical Orbits

We discuss a method to derive desired trajectories for follower (deputy) spacecraft from a single pre-determined desired trajectory (i.e., an orbit leader spacecraft) in a particular elliptical orbit. We assume that the desired trajectory can be obtained by using communications among neighbors in the network.

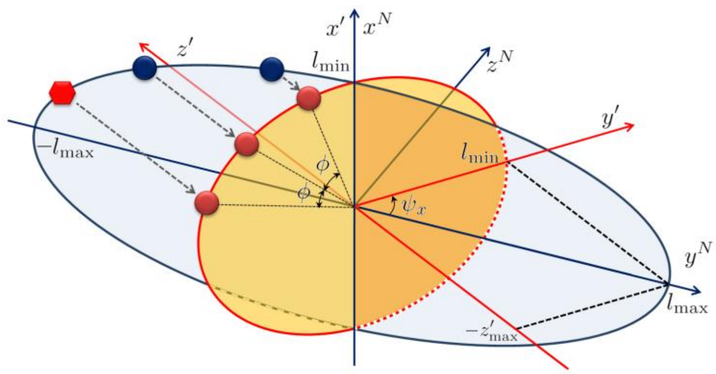

Fig. 2 Definition of $\boldsymbol{\psi_x}$ and the Relationship between the intermediate and the new frames

5.1 Coordinate Transformation in Elliptical Orbits

Although we have the desired trajectory in Eq. (4), the angle rotation using rotation matrices is difficult in ellipses. Therefore, by transforming the current frame to another, the elliptic orbit can be expressed by a combination of simple forms. In order to find the transformation matrix, we consider two consecutive coordinate transformations of the frame. The first transformation is to rotate the original frame to an intermediate frame such that the motion is expressed in a 2D motion, i.e., the orbit is located in the intermediate x - y plane (see Fig. 2). In this case, we should find positions for the maximum and minimum distances from the origin. The distance between the origin and the agent can be expressed from Eq. (4) as

$$l(\psi) = \sqrt{a_e^2 s^2_{(\psi-\psi_{e_0})} + 4a_e^2 c^2_{(\psi-\psi_{e_0})} + z_{\max}^2 s^2_{(\psi+\psi_{z_0})}} \tag{5}$$

where $\dot{\psi} = n(t)$ with the time-varying angular rate $n(t)$.
Differentiating Eq. (5) with respect to ψ yields the extrema of the distance.

$$\begin{aligned} \mathrm{d}l/\mathrm{d}\psi &= s_{(2\psi+2\Phi)}\sqrt{9a_e^4 + z_{\max}^4 - 6a_e^2 z_{\max}^2 c_{(2(\psi_{e_0}+\psi_{z_0}))}}\,/\,(2l) \\ \Phi &= 0.5\tan^{-1}\left((3a_e^2 s_{(2\psi_{e_0})} + z_{\max}^2 s_{(2\psi_{z_0})})\,/\,(-3a_e^2 c_{(2\psi_{e_0})} + z_{\max}^2 c_{(2\psi_{z_0})})\right) \end{aligned} \tag{6}$$

Hence, $l(\psi)$ has extrema for $\phi = -\Phi$ and $\phi = 3\pi/2 - \Phi$. That is, obtaining the positions of $l_{\min} = l(-\Phi)$ and $l_{\max} = l(3\pi/2 - \Phi)$, which are the $\hat{x}^N$ and $\hat{y}^N$ axes after the normalization, yields the first rotational matrix $\mathbf{R}_{\mathrm{nf}}$ as:

$$\mathbf{R}_{\text{nf}} = \frac{1}{l_{\min} l_{\max}} \begin{bmatrix} -l_{\max} a_e s_{(\Phi+\psi_{e0})} & 2l_{\max} a_e c_{(\Phi+\psi_{e0})} & -l_{\max} z_{\max} s_{(\Phi-\psi_{z0})} \\ -l_{\min} a_e c_{(\Phi+\psi_{e0})} & -2l_{\min} a_e s_{(\Phi+\psi_{e0})} & -l_{\min} z_{\max} c_{(\Phi-\psi_{z0})} \\ -2a_e z_{\max} c_{(\psi_{e0}+\psi_{z0})} & -a_e z_{\max} s_{(\psi_{e0}+\psi_{z0})} & 2a_e^2 \end{bmatrix} \tag{7}$$

The second rotation is related to finding an angle (ψ_x) with respect to the x^N axis such that the motion in the new x-y plane (i.e., x'-y' plane) becomes *circular*. One can notice from Fig. 2 that $l_{\min}$ becomes a radius of the circle in the new frame. Therefore, $\psi_x \geq 0$ can be expressed as

$$\psi_x = \cos^{-1}(l_{\min}/l_{\max}) \tag{8}$$

Figure 2 illustrates the definition of ψ_x and the geometrical relationship between the two frames. The second transformation matrix is defined as

$$\mathbf{R}_{\text{n1}}(\psi_x) := \begin{bmatrix} 1 & 0 & 0 \\ 0 & c_{\psi_x} & s_{\psi_x} \\ 0 & -s_{\psi_x} & c_{\psi_x} \end{bmatrix} \in \mathbb{R}^{3\times3} \tag{9}$$

Hence, the coordinate transformation from the original frame to the new frame can be found by combining Eqs. (7) and (9) as

$$\mathbf{q}'_d = (\mathbf{R}_{\text{n1}}(\psi_x)\mathbf{R}_{\text{nf}})\mathbf{q}_d =: \mathbf{R}_{\text{f}}\mathbf{q}_d \in \mathbb{R}^3 \tag{10}$$

where $\mathbf{q}'_d = [x'_d \quad y'_d \quad z'_d]^T$ and $\mathbf{q}_d = [x_d \quad y_d \quad z_d]^T$.

5.2 Phase Angle Shift Method in Elliptical Orbits

The proposed phase angle shift method enables spacecraft to shift their positions in elliptical orbits in 3D space simultaneously with only one phase shift angle ϕ. From the definition of an ellipse in Eq. (4), the direction of $\dot{\psi} = n(t)$ is *opposite* to that of $\dot{\phi}$ if the follower spacecraft are assumed to follow their orbit leader spacecraft. With this information, we consider motions in the x'-y' plane in advance. The angle rotation for the x'-y' plane can be expressed as

$$\begin{bmatrix} x'_{d,j} \\ y'_{d,j} \end{bmatrix} = \begin{bmatrix} c_{(j-1)\phi} & -s_{(j-1)\phi} \\ s_{(j-1)\phi} & c_{(j-1)\phi} \end{bmatrix} \begin{bmatrix} l_{\min} c_{(\psi+\Phi)} \\ -l_{\min} s_{(\psi+\Phi)} \end{bmatrix} = \mathbf{T}_{xy}((j-1)\phi) \begin{bmatrix} x'_d \\ y'_d \end{bmatrix} \tag{11}$$

For the phase angle shift in the z' axis, we define an auxiliary variable Z'_d as $Z'_d := z'_{\max} c_{(\psi+\Phi)}$ where $z'_{\max} = \sqrt{l_{\max}^2 - l_{\min}^2} \geq 0$. Then the angle rotation for z'_d and Z'_d can be defined as

$$\begin{bmatrix} z'_{d,j} \\ Z'_{d,j} \end{bmatrix} = \begin{bmatrix} c_{(j-1)\phi} & -s_{(j-1)\phi} \\ s_{(j-1)\phi} & c_{(j-1)\phi} \end{bmatrix} \begin{bmatrix} z'_{\max} s_{(\psi+\Phi)} \\ z'_{\max} c_{(\psi+\Phi)} \end{bmatrix} = \mathbf{T}_z((j-1)\phi) \begin{bmatrix} z'_d \\ Z'_d \end{bmatrix} \tag{12}$$

Hence, combining Eqs. (11) and (12) yields the proposed phase angle shift for the jth agent as

$$\mathbf{q}''_{d,j} = \underbrace{\begin{bmatrix} \mathbf{T}_{xy}((j-1)\phi) & \mathbf{0}_2 \\ \mathbf{0}_2 & \mathbf{T}_z((j-1)\phi) \end{bmatrix}}_{=:\mathbf{T}_{j-1}} \begin{bmatrix} \mathbf{q}'_d \\ Z'_d \end{bmatrix} =: \begin{bmatrix} \mathbf{q}'_{d,j} \\ z'_{\max} c_{(\psi+\Phi-(j-1)\phi)} \end{bmatrix} \tag{13}$$

where $\mathbf{0}_2$ is the 2×2 zero matrix and $\mathbf{T}_{j-1} = \mathbf{T}((j-1)\phi)$ denotes the phase angle shift matrix with $(j-1)\phi$ from the leader agent in the new frame.
The time derivative of the desired trajectory $\mathbf{q}''_{d,j}$ is used frequently in this paper:

$$\dot{\mathbf{q}}''_{d,j} = \mathbf{T}_{j-1}\dot{\mathbf{q}}''_d \in \mathbb{R}^4 \tag{14}$$

where $\dot{\mathbf{q}}''_d = [x'_d \quad y'_d \quad z'_d \quad Z'_d]^T$ with $\dot{Z}'_d = -z'_d \dot{z}'_d / Z'_d$.
Notice that the auxiliary variable Z'_d in Eq. (13) is purely used to apply the phase angle shift to z'_d. Thus, the auxiliary variable can be removed from the state vector after the rotation.

6. Robust Formation Control for Phase Synchronization in Swarms of Spacecraft

In this section, we introduce the adaptive phase synchronization controller. We begin with a transformation of the composite state variables with $\mathbf{R}_\mathrm{f}$ and $\mathbf{T}_{j-1}$.

6.1 Modification of States and Composite Variables

In Eqs. (10) and (13), we transformed the desired trajectory in the original frame ($\mathbf{q}_d$) to those in the new frame ($\mathbf{q}'_d$and $\mathbf{q}''_d$). For the transformation of $\mathbf{q}_j$, $\mathbf{R}_\mathrm{f}$ in Eq. (10) is used, i.e.,

$$\mathbf{q}'_j = \mathbf{R}_\mathrm{f}\mathbf{q}_j \tag{15}$$

From Section 5.1, the value of $\psi+\Phi$ can be obtained, which plays an important role when finding the auxiliary Z'_j in $q''_j = [x'_j \quad y'_j \quad z'_j \quad Z'_j]^T =: [\mathbf{q}'^T_j \quad Z'_j]^T$, which can be found as

$$Z'_j = z'_{\max,j}\, c_{(\psi+\Phi)} = R_{\mathrm{f},3}\mathbf{q}_j \cot(\psi+\Phi) \tag{16}$$

where $z'_{\max,j} = R_{\mathrm{f},3}\mathbf{q}_j / s_{(\psi+\Phi)}$ and $R_{\mathrm{f},3}$ is the third row vector of $\mathbf{R}_\mathrm{f}$.
From the definitions of $\mathbf{q}'_{d,j}$, $\mathbf{q}''_{d,j}$, $\mathbf{q}'_j$, and $\mathbf{q}''_j$ in Eqs. (10), (13), (15), (16), the modified composite variables ($\mathbf{s}'_j$, $\mathbf{s}''_j$) are obtained as well. The modified composite variable $\mathbf{s}''_j \in \mathbb{R}^4$ is written as follows:

$$\mathbf{s}''_j = \dot{\mathbf{q}}''_j - \mathbf{T}_{j-1}\dot{\mathbf{q}}''_d + \mathbf{\Lambda}''(\mathbf{q}''_j - \mathbf{T}_{j-1}\mathbf{q}''_d) \tag{17}$$

where $\mathbf{\Lambda}'' \in \mathbb{R}^{4\times 4}$ is a positive diagonal matrix, $\dot{q}''_j = [(\mathbf{R}_\mathrm{f}\dot{\mathbf{q}}_j)^T \ \dot{Z}'_j]^T$, and $\dot{\mathbf{q}}''_d = [(\mathbf{R}_\mathrm{f}\dot{\mathbf{q}}''_d)^T \ \dot{Z}'_d]^T$. The phase angle shift matrix $\mathbf{T}_{j-1}$ is defined in Eq. (13). The composite variable $\mathbf{s}'_j$ is directly obtained from the first three elements in $\mathbf{s}''_j$.

6.2 Phase Synchronization Controller

Given the dynamic models in Eq. (1) and the desired trajectories in Eq. (4), we should transform the original frame to the new frame by using the coordinate transformation $\mathbf{R}_\mathrm{f}$ in Eq. (10) such that we can use the phase angle shift method $\mathbf{T}_{j-1}$ in Eq. (13). By left-multiplying Eq. (1) by $\mathbf{R}_\mathrm{f}$ and $\mathbf{q}_j = \mathbf{R}_\mathrm{f}^T\mathbf{R}_\mathrm{f}\mathbf{q}_j = \mathbf{R}_\mathrm{f}^T\mathbf{q}'_j$, the dynamic models described in the new frame are written as

$$\begin{bmatrix} \mathbf{R}_\mathrm{f}\mathbf{M}_j(\mathbf{q}_j)\mathbf{R}_\mathrm{f}^T & \mathbf{0}_{3\times1} \\ \mathbf{0}_{1\times3} & (\mathbf{R}_\mathrm{f}\mathbf{M}_j(\mathbf{q}_j)\mathbf{R}_\mathrm{f}^T)_{3,3} \end{bmatrix}\ddot{\mathbf{q}}''_j + \begin{bmatrix} \mathbf{R}_\mathrm{f}\mathbf{C}_j(\mathbf{q}_j,\dot{\mathbf{q}}_j)\mathbf{R}_\mathrm{f}^T & \mathbf{0}_{3\times1} \\ \mathbf{0}_{1\times3} & (\mathbf{R}_\mathrm{f}\mathbf{C}_j(\mathbf{q}_j,\dot{\mathbf{q}}_j)\mathbf{R}_\mathrm{f}^T)_{3,3} \end{bmatrix}\dot{\mathbf{q}}''_j + \begin{bmatrix} \mathbf{R}_\mathrm{f}\mathbf{G}_j(\mathbf{R}_\mathrm{f}^T\mathbf{q}'_j) \\ G_{jZ'} \end{bmatrix} + \begin{bmatrix} \mathbf{R}_\mathrm{f}\mathbf{D}_j(\mathbf{R}_\mathrm{f}^T\mathbf{q}'_j, \mathbf{R}_\mathrm{f}^T\dot{\mathbf{q}}'_j) \\ D_{jZ'} \end{bmatrix} = \begin{bmatrix} \mathbf{R}_\mathrm{f}\boldsymbol{\tau}_j(t) \\ \tau_{jZ'} \end{bmatrix} \tag{18}$$

where $(\mathbf{R}_\mathrm{f}\mathbf{M}_j(\mathbf{q}_j)\mathbf{R}_\mathrm{f}^T)_{3,3}$ and $(\mathbf{R}_\mathrm{f}\mathbf{C}_j(\mathbf{q}_j,\dot{\mathbf{q}}_j)\mathbf{R}_\mathrm{f}^T)_{3,3}$ denote the (3,3) elements of $\mathbf{R}_\mathrm{f}\mathbf{M}_j(\mathbf{q}_j)\mathbf{R}_\mathrm{f}^T$ and $\mathbf{R}_\mathrm{f}\mathbf{C}_j(\mathbf{q}_j,\dot{\mathbf{q}}_j)\mathbf{R}_\mathrm{f}^T$, and $G_{jZ'}$ and $D_{jZ'}$ are defined by using the similar procedure in Eq. (16) as

$$G_{jZ'} = \mathbf{R}_{\mathrm{f},3}\mathbf{G}_j \cot(\psi+\Phi), \quad D_{jZ'} = \mathbf{R}_{\mathrm{f},3}\mathbf{D}_j \cot(\psi+\Phi) \tag{19}$$

In order to construct the proposed phase synchronization controller, the active parameter adaptation is introduced for the dynamic model in Eq. (1) for the purpose of tuning the tracking and diffusive coupling gains. The proposed formation control and phase synchronization controller for Eq. (1) including the nominal communication with the l th and m th agents can be written as:

$$\begin{aligned} \begin{bmatrix} \mathbf{R}_\mathrm{f}\boldsymbol{\tau}_j(t) \\ \tau_{jZ'} \end{bmatrix} &= \begin{bmatrix} \mathbf{R}_\mathrm{f}\mathbf{M}_j(\mathbf{q}_j)\mathbf{R}_\mathrm{f}^T & \mathbf{0}_{3\times1} \\ \mathbf{0}_{1\times3} & (\mathbf{R}_\mathrm{f}\mathbf{M}_j(\mathbf{q}_j)\mathbf{R}_\mathrm{f}^T)_{3,3} \end{bmatrix}\ddot{\mathbf{q}}''_{j,r} + \begin{bmatrix} \mathbf{R}_\mathrm{f}\mathbf{C}_j(\mathbf{q}_j,\dot{\mathbf{q}}_j)\mathbf{R}_\mathrm{f}^T & \mathbf{0}_{3\times1} \\ \mathbf{0}_{1\times3} & 0 \end{bmatrix}\dot{\mathbf{q}}''_{j,r} + \begin{bmatrix} \mathbf{R}_\mathrm{f}\mathbf{D}_j(\mathbf{R}_\mathrm{f}^T\mathbf{q}'_j, \mathbf{R}_\mathrm{f}^T\dot{\mathbf{q}}'_j) \\ \hat{D}_{jZ'} \end{bmatrix} + \begin{bmatrix} \mathbf{R}_\mathrm{f}\mathbf{G}_j(\mathbf{R}_\mathrm{f}^T\mathbf{q}'_j) \\ G_{jZ'} \end{bmatrix} \\ &\quad - k_1\mathbf{s}''_j + k_2(\mathbf{T}_{j-l}\mathbf{s}''_l + \mathbf{T}_{j-m}\mathbf{s}''_m) - \mathbf{W}_j(\mathbf{Ts}'', \varrho_j)\mathbf{c}_j - \alpha\mathbf{e}''_j \\ &= \begin{bmatrix} \mathbf{Y}_j(\mathbf{q}'_j, \dot{\mathbf{q}}'_j, \dot{\mathbf{q}}'_{j,r}, \ddot{\mathbf{q}}'_{j,r})\widehat{\mathbf{b}_j} \\ Y_{jZ'}\widehat{\mathbf{b}_j} \end{bmatrix} + \begin{bmatrix} \mathbf{R}_\mathrm{f}\mathbf{G}_j(\mathbf{R}_\mathrm{f}^T\mathbf{q}'_j) \\ G_{jZ'} \end{bmatrix} - \alpha\mathbf{e}''_j - k_1\mathbf{s}''_j + k_2(\mathbf{T}_{j-l}\mathbf{s}''_l + \mathbf{T}_{j-m}\mathbf{s}''_m) - \mathbf{W}_j(\mathbf{Ts}'', \varrho_j)\mathbf{c}_j \end{aligned} \tag{20}$$

where $k_1 > 2k_2 > 0$ for $p \geq 3$ [13], $\boldsymbol{\rho}_j = [\rho_{j1} \ \rho_{j2} \ \cdots \ \rho_{jp}]^T$, $\mathbf{Ts}'' = \{\mathbf{T}_{j-1}\mathbf{s}''_1, \mathbf{T}_{j-2}\mathbf{s}''_2, \cdots, \mathbf{T}_{j-p}\mathbf{s}''_p\}$, $\mathbf{T}_{j-i} = \mathbf{T}((j-i)\phi)$, and $\mathbf{e}''_j = \mathbf{q}''_j - \mathbf{q}''_{d,j}$. A constant $\alpha > 0$ is a design parameter and $\dot{q}''_{j,r} = [\dot{q}'^T_{j,r} \ \dot{Z}'_{j,r}]^T$ where $\dot{\mathbf{q}}'_{j,r} := [\dot{x}'_{j,r} \ \dot{y}'_{j,r} \ \dot{z}'_{j,r}]^T = \mathbf{R}_\mathrm{f}\dot{\mathbf{q}}_{j,r}$ with $\dot{\mathbf{q}}_{j,r} = \dot{\mathbf{q}}_{d,j} - \mathbf{\Lambda}(\mathbf{q}_j - \mathbf{q}_{d,j})$ and $\dot{Z}'_{j,r} = R_{f,3}\dot{\mathbf{q}}_{j,r}\cot(\phi+\Phi)$.

Detailed information for the gain adaptation ($\mathbf{c}_j$) and parameter estimation ($\hat{\mathbf{b}}_j$) can be found in [17]. Furthermore, the nonlinear stability proofs are derived in [17], which also shows that the synchronization error is smaller than the tracking error.

7. Numerical Validations

In this section, we evaluate the effectiveness of the proposed adaptive phase synchronization controller by simulating a reconfiguration of a swarm of spacecraft (S/C). The center of the LVLH frame is the position of the chief S/C described by the Proposition 1 in [14]. We can describe the motions of all S/C in the swarm by using Proposition 2 in [14]. In the simulation, we want to control the motions of 18 S/C in two orbits which are concentric ellipses in the same orbital plane. The initial positions of the S/C are randomly chosen with a uniform distribution with a range of $-0.5\,\mathrm{km} \le x_{j,0},\ y_{j,0},\ z_{j,0} \le 0.5\,\mathrm{km},\ j = 1,\cdots,18$. No initial velocity is assigned to all of the S/C. It is assumed that 6 S/C are placed in the inner orbit and the rest of them are in the outer orbit.

For simulations, the physical parameters are chosen as follows: $m_j = 100\,\mathrm{kg}$, $A_j = 1\,\mathrm{m}^2$, $C_D = 2.0$. The altitude of the chief S/C is $400\,\mathrm{km}$, and the initial classical orbital elements are $[a_0,\ e_0,\ i_0,\ \Omega_0,\ \omega_0,\ \nu_0] = [R_E + 400,\ 0,\ 45\,\mathrm{deg},\ 30\,\mathrm{deg},\ 0\,\mathrm{deg},\ 10\,\mathrm{deg}]$, where R_E denotes the radius of the Earth. The unmodeled disturbance $\mathbf{\Delta}_{\mathrm{dist}}$ including system's uncertainties is set as $\|\mathbf{\Delta}_{\mathrm{dist}}\| / m_j = 10^{-5}\,\mathrm{km/s^2}$.

The initial conditions of the desired trajectory for the orbit leader S/C are defined as: $x_{d,0} = 1\,\mathrm{km}$, $y_{d,0} = 1\,\mathrm{km}$, $z_{d,0} = 0.5\,\mathrm{km}$, $\dot{z}_{d,0} = 10^{-5}\,\mathrm{km/s}$. The values of $\dot{x}_{d,0}$ and $\dot{y}_{d,0}$ can be found by using the constraints in Eq. (4). For the controller in Eq.(20), the design parameters are set as follows: $k_1 = 3$, $k_2 = 1$, $\alpha = 1$, $\mathbf{\Lambda}_j = \mathrm{diag}(0.1, 0.1, \cdots, 0.1)$. For the gain adaptation law [17], $\mathbf{\Sigma}_j = \mathrm{diag}(10, 10, \cdots, 10)$, $c_{k,\max} = 1$, $\epsilon_{\mathbf{c}_j} = 1$. Initial values of the adaptive diffusive gains $\mathbf{c}_j$ are set to 0's. For the communication, no more than 5 connections with neighbors are allowed. The parameter estimation law is not used for simplicity and clarity of the performance of the proposed phase synchronization controller.

Figure 3 shows the trajectory motions for the S/C in 3D space during 900 s controlled by the proposed phase synchronization controller. Note that after reaching their orbits, S/C follow their desired trajectories without a drift. The first figure in Fig. 4 shows the trajectories of the 18 S/C in the swarm. Note that only x' (i.e., the first axis in the new frame (x' - y' - z')) was chosen because x', y', and z' have very similar results. In the figure, the trajectories are converging to each other regardless of their initial positions before approaching the desired trajectory individually. The contraction rate is obtained as $2\lambda = 0.002$. The estimated value of the maximum state error is $\|\delta \mathbf{q}_j\| = 0.5\,\mathrm{m}$ for individual S/C. The second figure in Fig. 4 shows the gains variations for the 7th S/C (the first one in the outer orbit) based on the gain adaptation law. The gains do not have values during 15 sec due to the zero initial conditions. Note that the 7th S/C has gains only for its neighbors in the same orbit (8th and 18th S/C) and those in the inner orbit (1st and 2nd S/C).

In order to evaluate the performance, we compare the proposed synchronization controller and the nominal gain-based controller with properly tuned gains. For the simulations, it is assumed that all S/C are initially located at the origin. The first figure in Fig. 5 shows the convergent time with respect to the size of the orbits (the number denotes the ratio to the orbit defined previously in this section.) with the same amount of fuel for reconfigurations. As the orbit size gets bigger, the proposed synchronization controller makes the S/C converge faster, which is due to the gain adaptation law. On the other hand, based on the same convergent time, the proposed synchronization controller uses less fuel consumption (ΔV) for the reconfiguration than the nominal gain-based controller (the second figure in Fig. 5).

Through the simulation results, we showed that the proposed phase synchronization controller more efficiently synchronized the motions of the spacecraft during the reconfigurations of the swarm.

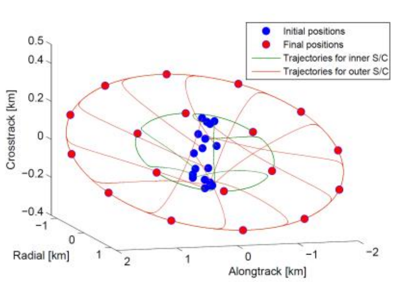

Fig. 3 Trajectories of the 18 S/C for 900s

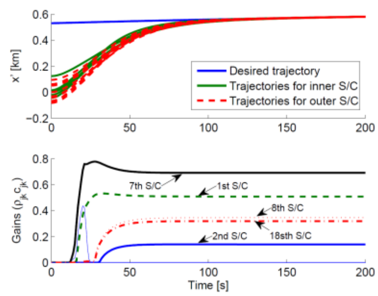

Fig. 4 Trajectories x'_j after transforming them to the position of x'_d (upper figure) and adapted diffusive gains for the 7th S/C

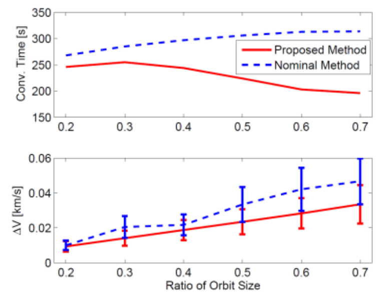

Fig. 5 Comparison of the performance: convergent time (upper figure) and fuel consumption (lower figure)

8. Conclusions

We presented a novel coordinate transformation method and a new phase synchronization control strategy for swarms of spacecraft constructed by the networked Euler-Lagrangian (EL) systems moving in elliptical orbits. The proposed coordinate transformation method and phase angle shift method facilitate the phase angle rotation in ellipses, thereby playing a crucial role in the phase synchronization control law. The proposed phase synchronization controller, which guarantees smaller error bound, robustly synchronize the motions of spacecraft with relaxed sensing topology for synchronization stability in the swarm.

Acknowledgements

The research was carried out in part at the Jet Propulsion Laboratory, California Institute of Technology, under a contract with the National Aeronautics and Space Administration. © 2011 California Institute of Technology. Government sponsorship acknowledged. The first author was supported by the University of Illinois at Urbana-Champaign. The authors gratefully acknowledge Dr. Lars Blackmore and Dr. Behcet Acikmese at JPL/NASA and Daniel Morgan at UIUC for their constructive discussion.

References

[1] M. Tillerson, G. Inalhan, J.P. How, Co-ordination and control of distributed spacecraft systems using convex optimization techniques, Int J Robust Nonlinear Contr, 12(2-3) (2002) 207-242.
[2] F.Y. Hadaegh, S.-J. Chung, H. Manaroha, Development and Flight of Swarms of 100-gram Satellites, IEEE Systems J (to be submitted).
[3] D.P. Scharf, F.Y. Hadaegh, S.R. Ploen, A Survey of Spacecraft Formation Flying Guidance and Control (Part I): Guidance, Amer Contr Conf, Denver, CO, (2003) 1733-1739.
[4] D.P. Scharf, F.Y. Hadaegh, S.R. Ploen, A Survey of Spacecraft Formation Flying Guidance and Control (Part II): Control, Amer Contr Conf, Boston, MA (2004) 2976-2984.
[5] R.W. Beard, J. Lawton, F.Y. Hadaegh, A Coordination Architecture for Spacecraft Formation Control, IEEE Trans Contr Systems Technol, 9(6) (2001) 777-790.
[6] P.K.C. Wang, F.Y. Hadaegh, K. Lau, Synchronized Formation Rotation and Attitude Control of Multi Free-Flying Spacecraft, J Guid, Contr, Dyn, 22(1) (1999) 28-35.
[7] W. Ren, R.W. Beard, Decentralized Scheme for Spacecraft Formation Flying via the Virtual Structure Approach, J Guid, Contr, Dyn, 27(1) (2004) 73-82.
[8] S.-J. Chung, U. Ahsun, J.-J.E. Slotine, Application of Synchronization to Formation Flying Spacecraft: Lagrangian Approach, J Guid, Contr, Dyn 32 (2) (2009) 512-526.
[9] R. Kristiansen, P.J. Nicklasson, J.T. Gravdahl, Spacecraft Coordination Control in 6DOF: Integrator Backstepping vs Passivity-Based Control, Automatica, 44 (2008) 2896-2901.
[10] J.R. Lawton, R.W. Beard, Synchronized Multiple Spacecraft Rotations, Automatica, 38(8) (2002) 1359-1364.
[11] R. Kristiansen, A. Loria, A. Chaillet, P.J. Nicklasson, Spacecraft Relative Rotation Tracking Without Angular Velocity Measurements, Automatica, 45 (2009) 750-756.
[12] M.S. de Queiroz, V. Kapila, Q. Yan. Adaptive Nonlinear Control of Multiple Spacecraft Formation Flying, J Guid, Contr, Dyn, 23(3) (2000) 385-390.
[13] S.-J. Chung, J.-J.E. Slotine, Cooperative Robot Control and Concurrent Synchronization of Lagrangian Systems, IEEE Trans Robot, 25(3) (2009) 686-700.
[14] I. Chang, S.-J. Chung, L. Blackmore, Cooperative Control with Adaptive Graph Laplacians for Spacecraft Formation Flying, 49th IEEE Conf on Decision and Contr, Atlanta, GA, (2010) 4926-4933.
[15] R. Olfati-Saber, R.M. Murray, Consensus Problems in Networks of Agents with Switching Topology and Time-Delays, IEEE Trans Autom Contr, 49(9) (2004) 1520-1533.
[16] W.H. Clohessy, R.S. Wiltshire, Terminal Guidance System for Satellite Rendezvous, J Aerospace Science, 27(9) (1960) 653-658.
[17] I. Chang, S.-J. Chung, F.Y. Hadaegh, Phase Synchronization Control of Robotic Networks on Periodic Ellipses with Adaptive Switching Topologies, AIAA Guid, Nav, Contr Conf, Portland, OR (2011) (accepted).